colorants

MDPI

Article

Sustainable Preservation of Medieval Greens Through Historical Reproduction and Spectroscopy

Magdalena Souto [1,2], Marcello Picollo [1,*], Giovanni Bartolozzi [1], Frédéric Jamme [3], Márcia Vieira [2,*], Paula Nabais [2] and Maria J. Melo [2,4,*]

[1] IFAC-CNR, Via Madonna del Piano 10, 50019 Sesto Fiorentino, Italy; magdalenasouto127@gmail.com (M.S.); g.bartolozzi@ifac.cnr.it (G.B.)
[2] LAQV/REQUIMTE, Department of Conservation and Restoration & of Chemistry, NOVA School of Science and Technology, 2829-516 Caparica, Portugal; p.nabais@fct.unl.pt
[3] Synchrotron Soleil, l'Orme des Merisiers, BP48 St. Aubin, 91192 Gif-sur-Yvette, France; frederic.jamme@synchrotron-soleil.fr
[4] Institute of Medieval Studies (IEM), NOVA University of Lisbon, Av. Prof. Gama Pinto, 1646-003 Lisboa, Portugal
* Correspondence: m.picollo@ifac.cnr.it (M.P.); mc.vieira@campus.fct.unl.pt (M.V.); mjm@fct.unl.pt (M.J.M.)

Abstract

By examining historical recipes from the medieval treatise The Montpellier *Liber Diversarum Arcium*, the creation of bottle green and verdigris pigments involved various types of tempera, such as parchment glue and gum arabic. Malachite was also prepared. These references and paints were analysed using infrared spectroscopy and visible spectroscopy techniques, such as micro-Infrared Spectroscopy (microFTIR) and Fibre Optic Reflectance Spectroscopy, (FORS) over the 350–1000 nm range. This research provided new insights into the pigments used in monastic manuscripts and Books of Hours, supported by valuable data from the Soleil synchrotron. Producing historically accurate reproductions and applying spectroscopy to analyse them promotes sustainable cultural heritage preservation by maintaining ancient artefacts, detecting early signs of degradation, and enabling the development of compatible restoration materials.

Keywords: medieval greens; micro-infrared spectroscopy (microFTIR); Fibre Optic Reflectance Spectroscopy (FORS); bottle green; verdigris; malachite; cultural heritage

1. Introduction

In this study, we aimed to advance the science of preserving and restoring medieval green pigments by preparing historically accurate reproductions and studying them using state-of-the-art techniques. We based our reproductions on recipes from an original treatise of the era and analysed them using infrared spectroscopy and vision region methods such as micro-Infrared Spectroscopy (microFTIR) and Fibre Optic Reflectance Spectroscopy (FORS) in the ultraviolet (UV), visible and near-infrared (NIR) regions. Promising results for bottle green were obtained using synchrotron deep-UV photoluminescence at the Soleil facility.

1.1. Medieval Copper Greens

Copper greens have been used as pigments since ancient times and remained popular until the 19th century. Over time, they were gradually replaced by viridian green, a hydrated chromium oxide ($Cr_2O_3 \cdot 2H_2O$ or $Cr_2O_3 \cdot nH_2O$), which became widely adopted,

Academic Editor: Anthony Harriman

Received: 9 February 2026
Revised: 18 March 2026
Accepted: 25 March 2026
Published: 7 April 2026

as shown in Figure 1 [1–11]. With the exception of malachite, a basic copper carbonate ($CuCO_3 \cdot Cu(OH)_2$), most other copper green pigments may have been synthesised during the medieval period [12–23]. Notable medieval copper greens include copper resinates and verdigris [24–45]; verdigris, in particular, is mainly composed of neutral copper acetate ($Cu(CH_3COO)_2\ H_2O$), as illustrated in Figure 2 [18].

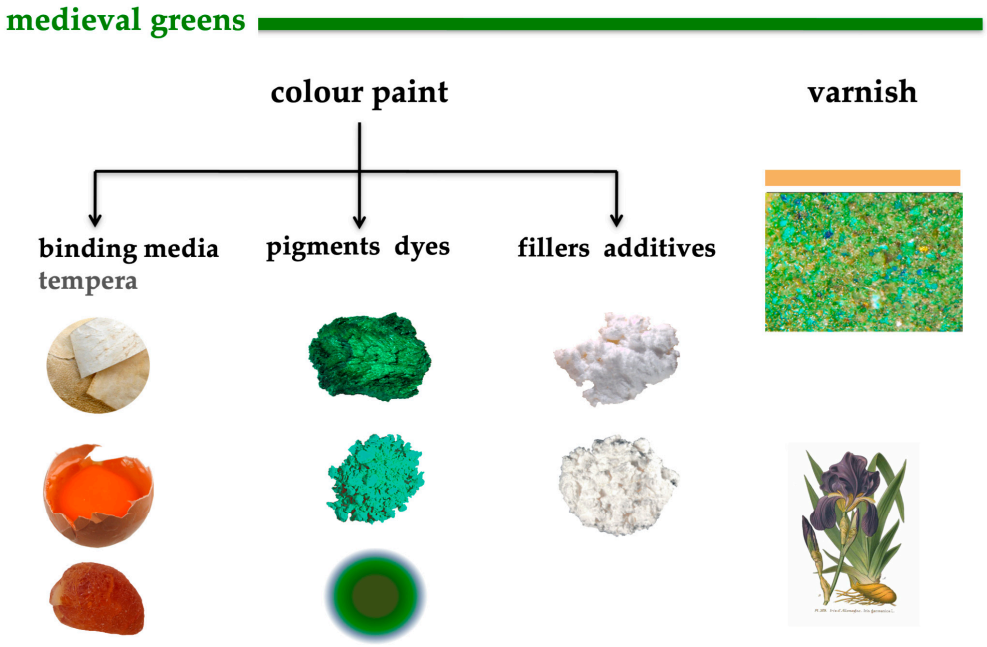

Figure 1. Medieval greens were made with substances like verdigris, iris juice, malachite, or copper sulfates. Tempera played a key role in preserving these paints, supported by fillers such as calcium carbonate or gypsum. All these materials were conclusively identified through a multi-analytical methods approach.

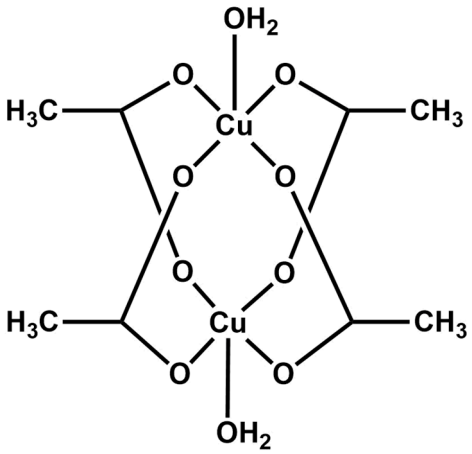

Figure 2. $Cu(CH_3COO)_2 \cdot H_2O$ represents a bridged carboxylate Cu^{2+} complex, also known as neutral copper acetate. The reproduction of 77 recipes confirmed that this was the main compound in verdigris [18].

Copper greens are an essential part of our medieval cultural heritage, appearing in objects such as artworks, manuscripts, and maps, as shown in Figure 3. Chemical sciences play a vital role in safeguarding these artefacts and in developing sustainable, innovative conservation techniques [1–23,45–48]. Currently, these materials face threats [6–10]; for example, in Portuguese monastic collections studied, 20% of the green areas are vulnerable to deterioration [34,35]. The use of verdigris on paper also poses significant challenges [12].

Its ageing process damages the organic support and causes the artwork's colour to shift from green to dark brown, significantly altering its appearance [1,4]. There is still much to learn about the degradation of neutral copper acetate [12].

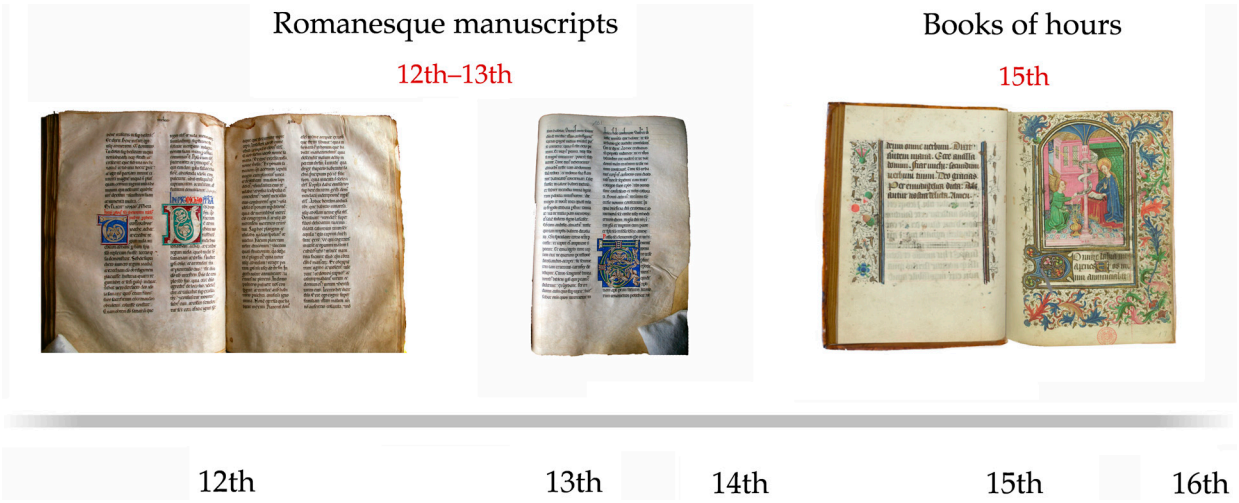

Figure 3. Medieval artefacts often feature copper green hues, such as the 12th–13th century Portuguese monastic collection, where bottle green was prominent. In the 15th century, simple copper sulfates also appeared in Books of Hours.

One of the most notable greens used in medieval manuscripts is bottle green, a synthetic copper proteinate. The first identification is likely in the magnificent *Book of Kells*. It was described by Doherty et al. as a copper-based green material, characterised using Raman and infrared spectroscopy [13]. However, the infrared spectra were obtained in reflection mode, so calcium oxalate (a degradation product of the tempera) was primarily identified. It is also found in an 11th–12th century codex produced at Fécamp Abbey (BnF Latin 5062; Coupry 1999, p. 76) [14,15], in Portuguese monastic works from the 12th–13th centuries [34], and in the scriptorium of Alfonso X, king of the Crown of Castile (r. 1252–1284) [37]. In the Portuguese monastic collections from the 12th to 13th centuries, the bottle green pigment remains bright and saturated. However, about 20% of it is detached from the support, likely caused by extensive chain scission and cross-linking in the medieval tempera binders. This is supported by the presence of calcium oxalate, a degradation product of the protein-based tempera. Chemometric analysis showed different levels of degradation in the bottle greens (Miguel 2012, pp. 85–104) [33]; for more details, see Section 1.2.2 below.

Other copper pigments have been identified in medieval artworks, such as basic copper sulfates found in illuminated manuscripts from the 15th century, as noted by Eremin et al. [10], and basic copper acetates mixed with chlorides and oxalates, also from the 15th century, found in paintings from Catalonia and the Crown of Aragon (oil and tempera), as studied by Salvadó et al. [8,9]. In this latter research, the authors are uncertain about the origin of these green compounds, particularly copper oxalates: were they applied as synthetic pigments or formed through the degradation of paint? Eremin et al. [10], in a detailed study of materials and techniques used in Islamic manuscripts, described various mixtures of copper greens to achieve subtle colour differences; they identified all the previously mentioned compounds and atacamite alone. These authors also discussed the origin of these greens, suggesting that they can be either artificially produced as copper corrosion products or as "natural mixtures resulting from the use of different ores." The primary analytical methods employed by Salvadó included X-ray diffraction (XRD), X-ray fluorescence (XRF), and infrared spectroscopy. Eremin's analyses involved Raman

microscopy and XRF. Earlier studies on copper greens, such as atacamite in paintings, were conducted by Naumova, Pisareva, and Nechiporenko in the 1990s; their characterization mainly involved transmitted light microscopy [11], and a basic copper sulfate found in 16th-century Russian frescoes was identified using XRD data.

1.2. Characterising Copper Greens and Their Degradation Products

1.2.1. Verdigris by Infrared Spectroscopy

Neutral copper acetate exhibits medium-strong infrared absorption bands at 3476, 3374, and 3272 cm^{-1}, corresponding to the OH stretching modes of water molecules associated with the acetate ion; see Figure 2 [18]. The weak bands at 2938 and 2941 cm^{-1}, which are characteristic of acetate spectra overall, correspond to the asymmetric and symmetric CH stretching modes, respectively [18,21]. In the fingerprint region, the main bands include the strong stretching absorption of the COO^- group at 1602 cm^{-1} and the absorption at 1445 cm^{-1}, attributed to CH_3 asymmetric bending, with a shoulder at 1421 cm^{-1} assigned to the symmetric stretching mode of the COO^- group [8,9,18,21,22]. Copper oxalates have mainly been linked to degradation products, with identification based on the asymmetric COO^- stretching mode at 1677 cm^{-1} and the symmetric COO^- stretching and bending modes at 1364 and 1320 cm^{-1} [8,23].

1.2.2. Bottle Green by Infrared Spectroscopy

Portuguese monastic artefacts containing bottle green pigments exhibit a prominent broad band near 1645 cm^{-1} in the fingerprint region. According to prior research [33], this band may result from the degradation of amide I and II bands of proteins around 1653 and 1540 cm^{-1}, along with an acetate band near 1635 cm^{-1} linked to copper pigments, indicating the formation of a copper proteinate complex. The protein matrix's OH and NH stretching bands form a distinctive pattern, with the NH band (~3350 cm^{-1}) showing reduced intensity (Miguel 2012, Figure 64 [33]). The C–H stretching region (3000–2840 cm^{-1}) also deserves attention. Calcium oxalate, a typical degradation product in medieval bottle green pigments, displays characteristic absorption bands at 1322 and 784 cm^{-1}. Principal Component Analysis (PCA) was vital for this study, applied to the C–H region (3000–2840 cm^{-1}) and the protein region (1770–1490 cm^{-1}) across 72 infrared spectra from bottle green paints from monasteries like Lorvão, Holy Cross, and Alcobaça. The PCA of the C–H data helped to differentiate scriptoria, revealing unique production traits for each manuscript. Additionally, a spectrum from a bottle green manuscript created at Fécamp Abbey's scriptorium (BnF Latin 5062, 1078–1108) was analyzed. Microscopic examination of an 11th–12th century manuscript from Fécamp's Benedictine Abbey showed the same infrared pattern in Portuguese Romanesque illuminations: the copper proteinate band near 1635 cm^{-1} and differences in the C–H stretching region (3000–2840 cm^{-1}), as demonstrated by PCA focusing on these spectral regions (Miguel 2012, Figures 66 and 67 [33]).

1.2.3. Malachite and Copper Sulfates by Infrared and Raman Spectroscopy

In the three Books of Hours examined at the National Palace of Mafra (ms 22, 23, and 24), dating from the 15th century, microspectroscopic techniques enabled identification of the elusive greens [42]. Infrared analysis confirmed that all three manuscripts predominantly contain a basic copper carbonate, which may be natural or synthetic malachite. For ms 22 and 24, malachite is mainly associated with basic copper sulfate and occasionally with lead-tin yellow, azurite, or both. Lead-tin yellow was also systematically employed to highlight brighter shades of green [42]. Raman microscopy indicated a mixture of brochantite and langite ($CuSO_4 \cdot 3Cu(OH)_2 \cdot 2H_2O$) [42]. The basic copper sulfates identified by Raman microscopy display characteristic bands at 973 and 910 cm^{-1}, corresponding to the SO_4^{2-} symmetric stretching vibration; the basic copper sulfate bands at 510, 482, and

450 cm^{-1}, with an additional band at 445 cm^{-1} in ms 24; and hydroxyl stretching vibrations exhibiting a characteristic doublet at 3568 and 3591 cm^{-1} for ms 22 and at 3565 and 3587 cm^{-1} for ms 24 [42]. Studies of miniature paintings featuring basic copper sulfates include posnjakite [7], $CuSO_4 \cdot 3Cu(OH)_2 \cdot H_2O$ (detected in nine of the 22 miniatures), and brochantite, $CuSO_4 \cdot 3Cu(OH)_2$ (found in two miniatures).

1.3. Use of Fibre Optic Reflectance Spectroscopy for Greens

This UV-VIS reflectance spectroscopy has been widely utilised as an in situ method for studying cultural heritage materials over many decades. Specifically, FORS, introduced in the 1980s [43], enables rapid in situ collection of hundreds of reflectance spectra, aiding in the characterization of artist materials. Initial applications of the FORS technique were limited to the visible region, but over time, the operating range has expanded significantly. Currently, FORS can cover the entire UV-NIR range with various instrument setups. As the spectral range extends further into the NIR region, the likelihood of identifying materials beyond those present at the surface increases. Portable systems, equipped with fibres, can gather a significant amount of information. The main limitations of FORS include difficulty in analyzing spectral responses from mixtures of substances (such as combinations of colourants); poor spectral responses in artworks or samples with irregular surfaces or partial transparency; and the challenge of distinguishing colourants with similar absorption characteristics. In such cases, the combined use of other analytical methods becomes essential.

Although FORS is now widely adopted in research and cultural heritage conservation, publicly accessible FORS spectral databases remain limited. The first such database was developed by CNR-IFAC in 2002 and currently comprises several datasets acquired with different instruments and configurations. These datasets include reflectance spectra of a broad range of reference materials and substrates—such as paintings on wood, canvas, paper, and coloured textile fibres—collected under various measurement conditions (https://spectradb.ifac.cnr.it/index.php; accessed on 24 March 2026). Another notable online resource is the FORS database kept by CHSOS, which covers the spectral range of 350–950 nm and is accessible at https://chsopensource.org/products/reflectance-spectroscopy/reflectance-spectroscopy-system/fors/; accessed on 24 March 2026.

1.4. Recipes for Copper Greens in the Medieval Treatise the Montpellier Liber Diversarum Arcium

The Montpellier *Liber Diversarum Arcium* is one of the most comprehensive art treatises from the 14th century [26]. The only surviving copy is in the Montpellier Manuscript (MS H 277), housed in the medical section of the Interuniversity Library of Montpellier, France. This manuscript is classified among medical texts, likely copied for or by a physician around 1400–1430 in northern Italy. The original version of the treatise was clearly designed for practical use by painters [26].

With its thirty recipes, section §1.16, dedicated to verdigris, is undoubtedly the most extensive in the *Liber Diversarum Arcium*. The verdigris section is divided into two parts: the first, called "Greens," covers the preparation of powdered pigment; the second explains how to produce verdigris tempera using various binders and additives.

In a brief overview of different types of greens, this section mentions greens from Greece, Spain, and Rouen, as well as the pigment called "green-salt". Recipes §1.16.2–12 discuss how to make the pigment, including a subsection on creating Calcucecumenon, also known as "burnt copper," in recipes § 1.16.6–9. Recipes § 1.16.13–30 describe how to prepare tempera paints based on verdigris.

There are many comments on high-quality tempera, along with advice on which type of tempera works best with different media. Examples include tempera used as writing ink,

as well as more transparent types and those that last longer. The pigment recipes mainly list two key ingredients: metallic copper and vinegar. Depending on the recipe, additives like salt, honey, or soap may also be used. Tempera paints always contain powdered pigment, a gum-based binder such as gum arabic, and a solvent, which can be vinegar or wine. Many recipes also include an organic ingredient—usually a yellow plant or flower extract—to adjust the hue and give it a warmer, more natural tone.

2. Materials and Methods

2.1. Preparation and Selection of the Paints

From section §1.16 of the *Liber Diversarum Arcium*, focused on verdigris, one recipe was selected for producing the powdered pigment and another for preparing tempera [26]. These choices were based on their practicality and the likelihood of successful reproduction. The pigment recipe selected was § 1.16.10, which involves suspending copper foil in vinegar vapour. It was chosen because it produces a pure form of copper acetate, a key component of verdigris.

For the tempera, a variety of recipes are presented, each with distinct features. Some use vinegar as a solvent, while others substitute it with wine. Adding saffron to adjust the colour is recommended, along with other yellow organic extracts from plants such as elderberry, cabbage, or *Reseda luteola*. Some recipes require over a week of preparation, while others are ready to use immediately. A recipe with a clear structure, an average preparation time, and ingredients representative of the section's diversity was needed. Ultimately, the most suitable choice was §1.16.17.

To follow the recipes, greens were purchased from Kremer Pigmente—Aichstetten, Germany (malachite chiara); from Panreac—Castellan del Vallès, Spain (verdigris); and from Zecchi, Firenze, Italy (malachite). Gum arabic was bought from Kremer, #63300. The pieces were crushed to a powder in an agate mortar with a pestle and then dissolved in Millipore water to prepare a 15% solution (Lisbon, Portugal). Portuguese white wine, "Vinho Regional Minho Branco, Amesmla", 9.5° alcohol and commercial white wine vinegar, 6%, Espiga, were used as solvents. Gelatine was from a commercial brand Jerónimos® (Pingo Doce supermarket, Caparica, Portugal). The final paints were applied to filter paper.

Following these recipes sometimes required the researchers to "fill in the gaps" where various steps were not clearly stated in the treatises, possibly because these steps were implicit at the time or because information was lost during the manuscript copying process. Additionally, determining the ingredient quantities involved translating them into a language understandable today, so that the recipes could be reproduced unambiguously.

Detailed data on the preparation of these paints, as historical references, are described in Tables 1 and 2. The paints were applied in 2 cm-by-2 cm squares. The optimal choices are also listed in Tables 1–3.

For the tempera recipe, §1.16.17, the listed ingredients included gum arabic, white wine vinegar, wine, verdigris powder, and the juice of a green or yellow plant. Gum arabic, white wine vinegar, wine, and verdigris were straightforward to find. For the organic extract, *Reseda luteola* was selected, a plant often associated with verdigris. The weld solution was prepared by adding 0.3 g of weld to 20 mL of Millipore water and then heated to 90 °C for 1 h with constant stirring. The solution was subsequently filtered. The recipe steps are as follows: dissolve the gum arabic in a previously boiled wine or vinegar solution; crush the verdigris onto a stone (an agate mortar was used for this study); wet the pigment with the solvent and dissolve it; add the gum arabic solution to the powdered pigment; and then allow the tempera to dry for three days. To revitalise the tempera, the selected solvent was added; finally, the previously prepared organic extract was incorporated to adjust the colour, transforming it from a very cold green to a warmer, more natural hue.

Table 1. Verdigris paints. A 15% solution of gum arabic (GA) was prepared with each solvent. Extracts prepared with *Reseda luteola* were also added to two paints (weld).

Name	Paint Preparation	Revitalization	Paint
verdigris 1	0.5 g verdigris in 0.5 mL water 2.5 mL of a 15% GA/water	2 mL gum water + 0.5 mL water	
verdigris 2a	1.03 g verdigris in 1 mL vinegar 7 mL of a 15% GA/vinegar	3 mL wine	
verdigris 2b	1.02 g verdigris in 1 mL vinegar 4 mL of a 15% GA/vinegar	2.5 mL vinegar 1 mL wine + 1 mL of weld	
verdigris 3a	1.03 g verdigris in 1.5 mL wine 5 mL of a 15% GA/wine	3 mL wine	
verdigris 3b	1.03 g verdigris in 1.5 mL wine 5 mL of a 15% GA/wine	2.75 mL wine + 0.75 mL of weld	

Table 2. Bottle green paints. The preparation of the bottle green involved using a 10% gelatine solution and extracts prepared with *Reseda luteola* (weld).

Name	Paint Preparation	Revitalization	Paint
bottle green (I)	1 g verdigris in 1.5 mL vinegar 5 mL 20% GA solution added to the vinegar	1.0 mL of vinegar *final paint* 1 mL verdigris paint + 1 mL of weld extract + 4 mL of 10% gelatine solution	
bottle green (II)	1 g verdigris in 1.5 mL vinegar 5 mL 20% GA solution added to the vinegar	1.5 mL of vinegar *final paint* 0.5 mL verdigris paint + 0.5 mL of weld extract + 4 mL of 10% gelatine solution	
bottle green (III)	1.02 g verdigris in 1 mL vinegar 4 mL 15% GA solution added to the vinegar	2.5 mL vinegar; + 1 mL of weld; 1 mL vinegar *final paint* 1 mL verdigris paint + 0.75 mL of weld extract + 4 mL of 10% gelatine solution	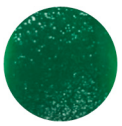
bottle green (IV)	1.03 g verdigris in 1.5 mL of white Portuguese wine + 5 mL of a 15% GA/wine solution	2.75 mL of wine + 0.75 mL of weld *final paint* 1 mL verdigris paint + 1 mL of weld extract + 4 mL of 10% gelatine solution	

Table 3. Preparation of malachite paints. The paints were prepared with a 15% solution of gum arabic (GA). Millipore water was used.

Name	Pigment	Revitalization	Paint
malachite clear	1 g malachite in 1.5 mL water 3 mL of a 15% GA	0.5 mL of Millipore water 1 mL of GA	
malachite Zecchi	0.5 g malachite in 0.5 mL water 3 mL of a 15% GA	1 mL of GA 0.5 mL water	

Regarding the quantities, Tables 1 and 2 show the proportions used. The preparation of the bottle of green paint involved the following steps: the first part consisted of dissolving verdigris in vinegar or wine, followed by the addition of a gum arabic solution. Then, 1 mL of the dissolved verdigris was added to 4 mL of a solution of 10% gelatine under constant stirring and heating at 40 °C. Finally, the yellow weld extract was added, resulting in the bottle green paint.

Preparation of malachite paints: The malachite layers were prepared by moistening 1.00 g of pigment with distilled water and allowing it to dry overnight. Then, 3.00 mL of a 15% gum arabic solution in water was added. The clear malachite dispersed very quickly in water. In contrast, the Zecchi malachite was more challenging to prepare due to the larger grains, which remained clumped together instead of dispersing smoothly. This resulted in the clear malachite forming a uniform tempera that was easy to apply and provided good coverage. Conversely, the Zecchi malachite produced an uneven tempera, making it challenging to use on the selected paper filter supports. See Table 3 for details.

2.2. Microscopy

The micro-sampling was conducted under a Leica MZ16 stereomicroscope equipped with a Leica ICD digital camera and a fibre-optic light Leica system (Leica KI 1500 LCD) acquired by the Schott technology group, Lisbon, Portugal. A set of 10 ocular lenses and objectives, with magnifications ranging from 0.71× to 11.5×, provided a total resolution range of 7.1× to 115×. The micro-samples were collected using a micro chisel nº13603 attached to a micro graver oval nº13611, both from Ted Pella® (Ted Pella Inc, Riverside, CA, USA).

Studying cultural heritage, whether through micro-samples or micro-analytical techniques (in situ or on samples), involves understanding the connection between a small sample and the larger, inherently heterogeneous artwork. Therefore, using in situ imaging and microscopic examination prior to sampling is crucial. Since artwork samples are unique and analytical techniques are continuously improving, future scientific advancements will enhance our ability to preserve cultural heritage [45]. Often, answering vital conservation questions involves careful sampling and selecting suitable analytical methods, especially when on-site instrument access is limited. Globally, conservation scientists strive to address issues that maintain object integrity; micro-sampling, which can provide valuable insights with minimal visible damage, is sometimes essential. Much of our understanding of historical materials comes from microscopy and micro-analytical studies [46]. Our micro-samples, which are invisible to the naked eye, were collected after detailed examination of the manuscripts between 2004 and 2013. These samples are stored in polypropylene cabinets and kept on glass slides at 20 °C.

2.3. Fibre Optic Reflectance (FORS)

Two Zeiss spectroanalyzers (Oberkochen, Germany)—models MCS 601 UV-NIR and MCS 611 NIR 2.2 WR—were employed to cover the spectral ranges of 190–1000 nm and 910–2200 nm, respectively. The MCS 601 features a spectral sampling interval of 0.8 nm/pixel over the 190–1000 nm range and utilises a linear array of 1024 silicon photodiodes. The MCS 611, operating with a sampling step of approximately 6 nm/pixel, is equipped with a linear array of 256 InGaAs photodiodes. Both spectroanalyzers are integrated into a single chassis, along with a 10 W halogen light source (model CLH600) characterised by a colour temperature of approximately 3000 K and an emission range of 320–2500 nm. Quartz optical fibres and a custom-designed 8°/8° probe head developed by CNR-IFAC were used to direct and collect the backscattered radiation. This probe head enables analysis of a spot approximately 2 mm in diameter. Instrument calibration was performed using a 99% reflective Spectralon® standard. Spectral data were acquired in the 350–2150 nm range; however, due to the limited spectral features in the NIR region—primarily corresponding to absorption bands of the paper substrate—only the 350–1000 nm range is presented and discussed in this study.

2.4. Micro-Infrared Spectroscopy (microFTIR)

Infrared analyses were performed using a Nicolet Nexus spectrophotometer coupled to a Continuμm microscope (15× objective) with an MCT-A detector. The spectra were collected in transmission mode, in 50 μm^2 areas, resolution setting 4 or 8 cm^{-1} and 128 scans, using a Thermo diamond anvil compression cell, which were subsequently converted to absorption. CO_2 absorption at ca 2400–2300 cm^{-1} was removed from the acquired spectra (4000–650 cm^{-1}). To improve the robustness of the results, at least two spectra were acquired from different sample spots. The microFTIR device was manufactured by ThermoNicolet in the USA and installed by Unicam Sistemas Analíticos Lda.

2.5. Synchrotron Deep UV Photoluminescence

Using the POLYPHEME and TELEMOS end-stations of the DISCO imaging beamline of the SOLEIL synchrotron facility (proposal 20221751), Deep UV (DUV) excitation was achieved at 240 to 300 nm with an acquisition emission range between 260 and 900 nm [49]. The POLYPHEME end-station was used to perform hyperspectral photoluminescence micro-imaging and to acquire full emission spectra with high spectral resolution. Emission spectra were recorded on an Olympus IX71 inverted microscope with lens replacement to be transparent in the deep UV range, a 40 × Zeiss Ultrafluar UV-transmitting immersion objective, using a 280 nm dichroic filter which acts as a beam-splitter, exciting at 270 nm and collecting between 450 and 700 nm. Raster scanning maps were collected with integration times of 5 s (1 accumulation) in areas between 280 μm^2 and 1.25 mm^2 using 2 to 15 μm steps. References and microsamples were analysed between two 170 μm quartz coverslips (UV fused silica, ESCO Optics, Oak Ridge, TN, USA). Data were acquired and processed using the Labspec6 software (Horiba, Palaiseau, France). The TELEMOS end-station was used for wide-field luminescence microscopy. Excitation was carried out at 250 and 270 nm. The TELEMOS end-station was used for wide-field luminescence microscopy. Images were collected using an Axio ObserverZ1 microscope (Carl Zeiss MicroImaging, BANGS Laboratories, Fishers, IN, USA) with a 40 × Zeiss Ultrafluar UV-transmitting immersion objective, using a 300 nm dichroic filter and setting the excitation at 270 nm. Fluorescence was collected using four emission bandpass filters, selected on the basis of the main spectral features observed with POLYPHEME: 329–351 nm; 412–438 nm; 510–560 nm; and 600–650 nm (IDEX, Semrock optical filters, Rochester, NY, USA). Acquisition time was

set to 30 s for each channel. The images obtained were also processed using the ImageJ software Java 8.

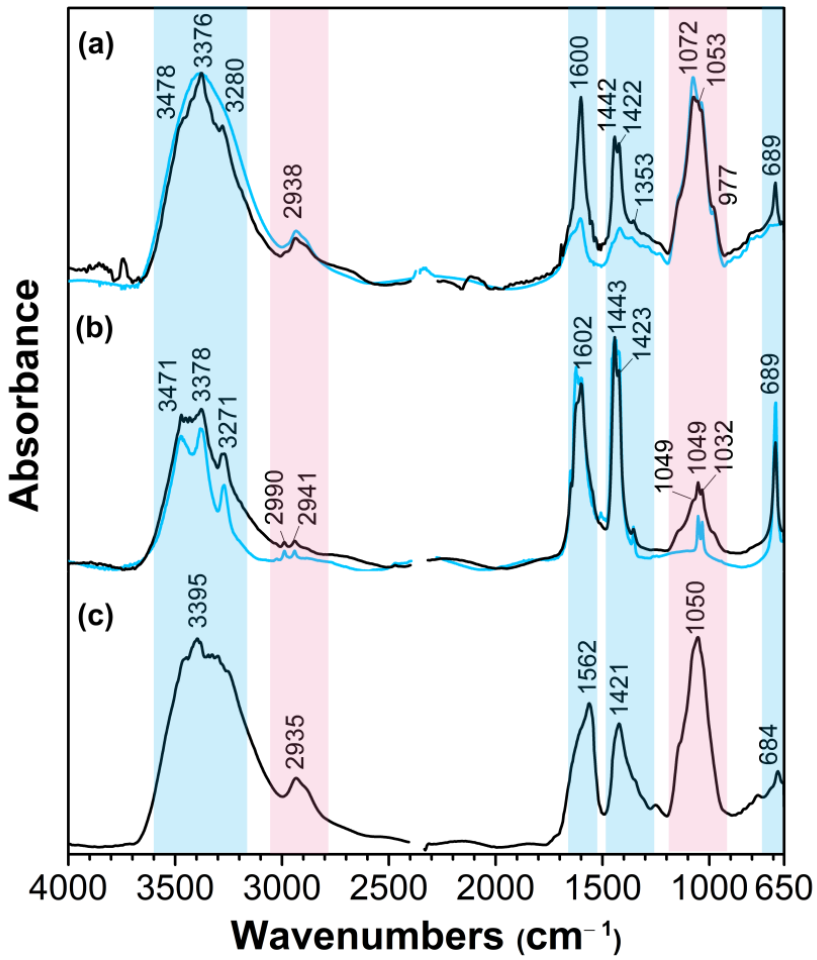

Figure 4. Verdigris was tempered with three different solutions: (**a**) with water (black) and gum arabic reference (blue); (**b**) with vinegar (black) and verdigris reference (blue); and (**c**) with wine. The blue bands indicate the bands corresponding to verdigris and the O–H from gum arabic, while the light pink ones show the areas where both verdigris and the gum arabic bands are identified.

3. Results

3.1. Infrared Spectra

3.1.1. Infrared Spectra for Verdigris

Figure 4 shows the FTIR spectra of verdigris tempera paints in gum arabic using three different solvents (water, vinegar, and wine), compared with verdigris powder (based on neutral copper acetate) and gum arabic. Gum arabic is present in high quantities. It displays a broad band at around 3383 cm^{-1} due to O–H stretching, a weaker yet visible band at 2933 cm^{-1} in the CH region, and the fundamental fingerprint region at 1074–76, 1038, and 981 cm^{-1}, corresponding to the bending of C–O–C bonds. For more information, please see Vieira et al. [38] (pp. 15–18). Comparing the spectra of the tempera paints with that of copper acetate, we see that the pigment's characteristic absorption bands are identifiable in the water- and vinegar-based samples. This is not the case for the wine-based tempera, which shows a different pattern, particularly in the region between 1650 and 1350 cm^{-1}. Notably, a band at 1562 cm^{-1} appears in this spectrum, which is absent in the others. All spectra show significant amounts of gum arabic, with the vinegar-based tempera having the lowest amount and the wine-based tempera the highest.

3.1.2. Infrared Spectra of Medieval Bottle Green

Figure 5 shows the infrared spectra of bottle green and gum arabic. Bottle green is prepared with various components, such as gum arabic, a protein (gelatin), verdigris tempera (which, when mixed with gelatin, forms a new copper-based compound: copper proteinate), and *Reseda luteola* extract. The spectrum displays a broad band around 3350 cm^{-1}, associated with the stretching of the OH group in the protein and gum arabic structures. In the fingerprint region of the proteinaceous tempera, it features two strong absorption bands at 1649 and 1555 cm^{-1}, representing amide I and II, respectively, and at 1442 cm^{-1} attributed to C-N bond stretching. The bands at 2935 and 1072 cm^{-1} correspond to the stretching of CH_3 and C–O–C bonds in gum arabic, respectively.

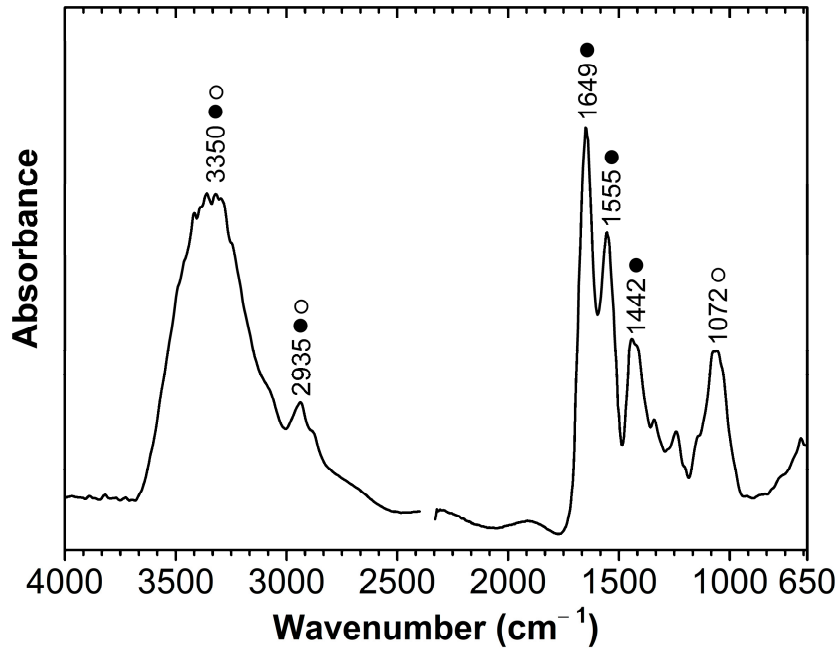

Figure 5. Infrared spectra of bottle green (III) with the bands of the protein (●) and of the gum arabic (○) indicated.

In Miguel's doctoral thesis from 2012 (pp. 85–104, Figure 64 in [33]), spectra of bottle green were obtained through the analysis of medieval Portuguese manuscripts. These spectra, along with the absorption bands of previously discussed components, also revealed signals associated with other copper compounds such as oxalates, in addition to proteinate. Most of these bands mainly originate from proteins and polysaccharide ligands.

3.1.3. Infrared Spectra of Malachite

Figure 6 shows the spectra of clear malachite, gum arabic, and malachite in gum arabic; see Table 3. The infrared spectrum of malachite displays four very strong absorption bands associated with carbonate (CO_3^{2-}) groups in the regions 1390–1500 cm^{-1} (ν3 antisymmetric stretching), 800–900 cm^{-1} (out-of-plane bending), 680–780 cm^{-1} (in-plane bending), and 1000–1100 cm^{-1} (symmetric stretching). All basic carbonates also show fundamental OH group stretching modes; for malachite, signals are observed between 3400 and 3320 cm^{-1}. Malachite tempera combines the spectra of the pure pigment and the binder. The presence of gum arabic influences the intensity and shape of the bands but does not prevent the recognition of the pigment's characteristic absorption patterns.

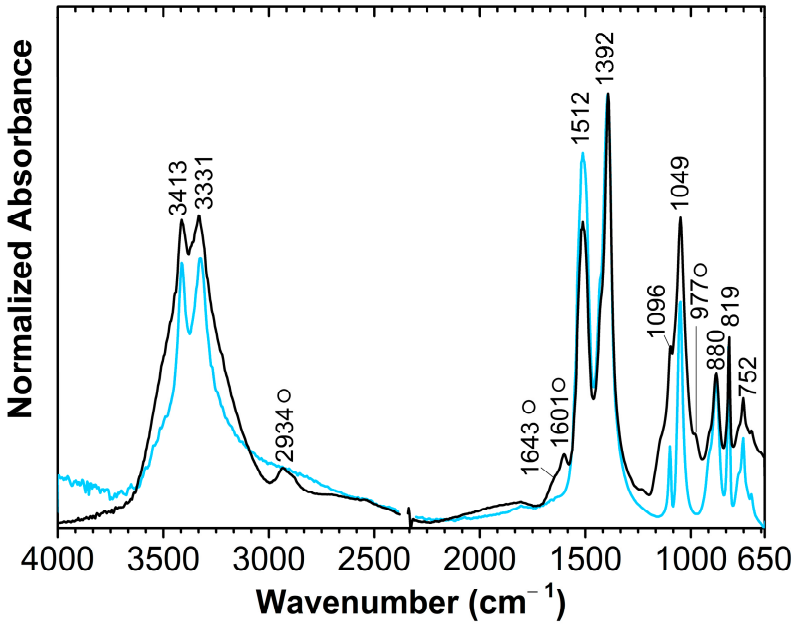

Figure 6. Infrared spectra of malachite paint (black) and a malachite reference (blue) with the bands of the gum arabic (O) indicated.

3.2. FORS Analysis of Paints Based on Verdigris, Malachite, and Bottle Green

The reflectance spectra of copper-based greens are generally characterised by a reflectance maximum in the blue–green region, accompanied by two principal absorption bands located in the UVa–violet (300–420 nm) and red–near-infrared (600–1300 nm) regions, Figures 7–9. Unlike other spectroscopic methods, the reflectance spectra of pure materials acquired by FORS in the visible range can be significantly influenced by the presence of mixtures or surface glazes involving other compounds. Such interactions can modify the perceived colour of the material, affecting both hue and saturation. As a result, the reflectance maximum of a given material may exhibit notable variations in intensity and, in some cases, wavelength shifts. Therefore, material identification using FORS must also consider the precise positions of its diagnostic absorption features. This becomes particularly critical when analysing mixtures of coloured compounds (i.e., pigments or dyes, excluding black and white materials), where their relative concentrations can induce shifts in the absorption maxima. These shifts are challenging to predict without prior knowledge of the component concentrations and the thickness of the paint layer.

As reported in Figure 7, verdigris exhibits two main absorption bands in the 350–420 nm (UVa–violet/blue) and 600–1000 nm (red–NIR) regions. The former corresponds to LMCT transitions from the pπ orbitals of oxygen atoms in acetate groups to the *d* orbitals of Cu^{2+} [43,44]. The second absorption band, centred at approximately 730 nm, is attributed to d–d ligand field transitions of the Cu^{2+} ion [43]. The absorption band exhibits variations in shape, intensity, and width across the different references. These differences may be attributed to factors such as variations in pigment concentration, layer thickness, and the specific materials used in the preparation of the tempera paints. As shown in Table 1, the five references display slight differences in hue, which are reflected in the position of the reflectance maximum. This maximum spans from approximately 490 nm (verdigris 1), typically associated with cyan hue, to around 520 nm (verdigris 2b and 3b), corresponding to a cooler green tone.

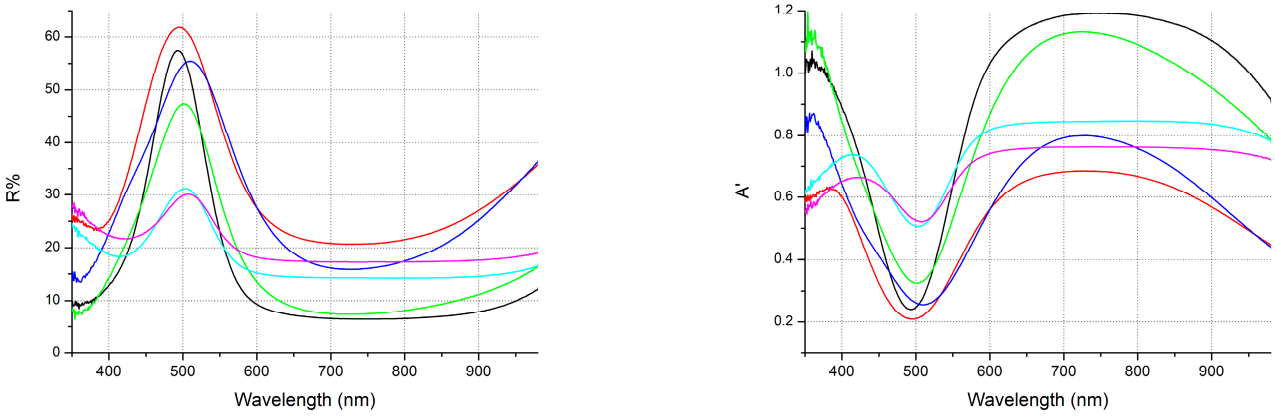

(**a**) (**b**)

Figure 7. Reflectance (**a**) and apparent absorption (**b**) FORS spectra of verdigris references. Verdigris 1 (black, two layers); verdigris 2a (red, five layers); verdigris 2b (green, three layers); verdigris 2b (blue, five layers); verdigris 3a (cyan, three layers); verdigris 3b (magenta, three layers).

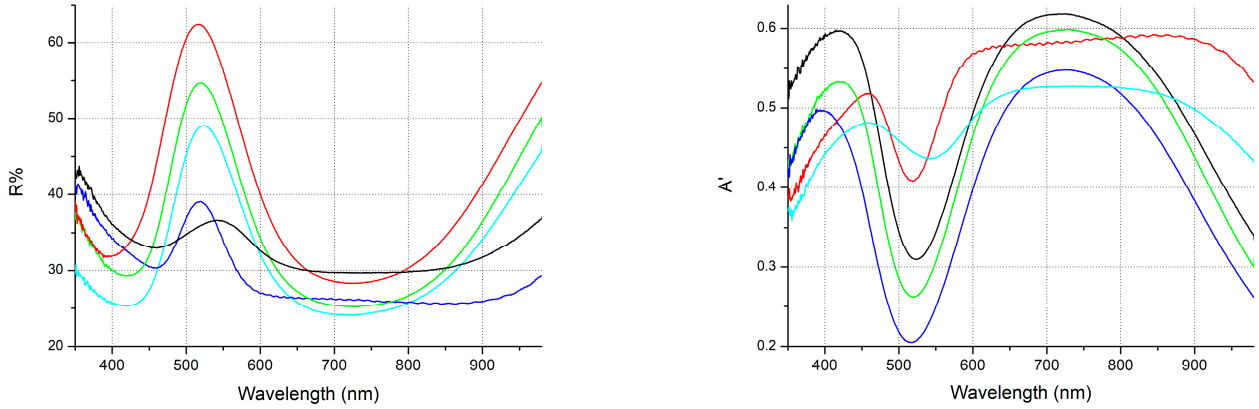

(**a**) (**b**)

Figure 8. Reflectance (**a**) and apparent absorption (**b**) FORS spectra of bottle green references. Bottle green I (cyan); bottle green II (blue); bottle green III (green, two layers); bottle green III (red, five layers); bottle green IV (black).

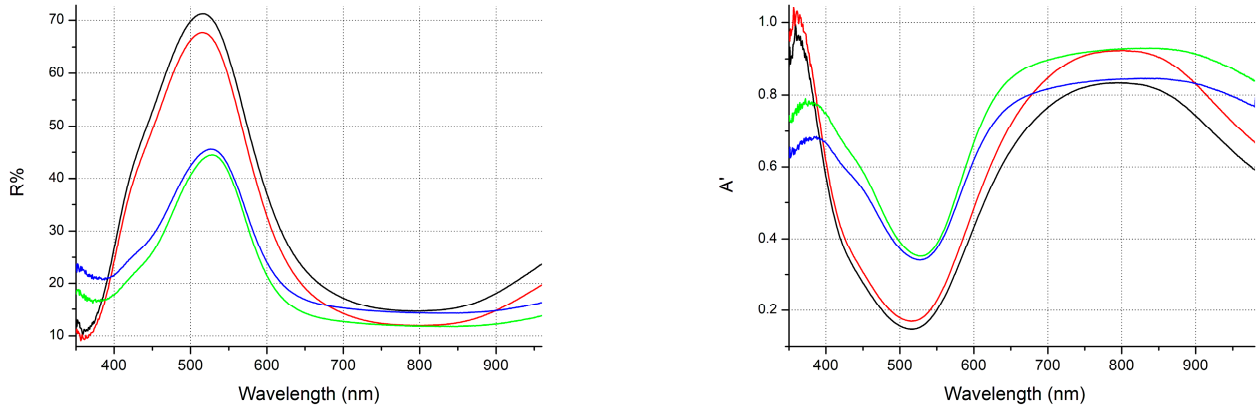

(**a**) (**b**)

Figure 9. Reflectance (**a**) and apparent absorption (**b**) FORS spectra of malachite references. Malachite MC (black, two layers); malachite MC (red, five layers); malachite MZ (green, two layers); malachite MZ (blue, five layers).

For malachite, the absorption band observed in the 600–1400 nm region, centred approximately at 800 nm, is attributed to *d–d* ligand field transitions of the Cu^{2+} cation; see Figure 9. In addition, it presents a shoulder at around 465 nm. In contrast, the absorption feature in the UVa–violet region (approximately 375 nm) is associated with ligand-to-metal charge transfer (LMCT) transitions [43].

The two malachite references exhibit nearly identical reflectance spectra, with only slight differences in the position of the reflectance maximum. These variations are attributed to differences in the paint layer preparation. Specifically, the Zecchi malachite (MZ), characterised by a slightly coarser grain size, produced a grainier tempera paint, resulting in a different surface texture and a subtly altered final colour compared to the other malachite (MC).

Based on the results obtained, distinguishing among the three green pigments using FORS within the spectral range considered in this study is challenging. However, malachite can generally be differentiated from verdigris and bottle green by its distinct spectral profile, with a shoulder at approximately 465 nm and a red-shifted absorption maximum near 800 nm, compared to the 700–740 nm range observed for the other two pigments. Verdigris and bottle green exhibit highly similar spectral features in the red to near-infrared region, Figures 7 and 8. The presence of the yellow dye in bottle green introduces a spectral variation in the cyan region of the reflectance maximum. However, this effect is comparable to that observed when verdigris is mixed with diverse yellow dyes or pigments during paint application.

3.3. Comparison with Medieval Greens in the Monastic World and Books of Hours

Bottle green was a significant colour in the monastic world during the 12th and 13th centuries century. Being a synthetic copper proteinate, the main component identified in the infrared spectra of bottle green is the protein, though with important changes; see Figure 10. In most of the spectra obtained from the Portuguese bottle green paints, what is observed is a broad band at approximately 1650 cm^{-1}, as can be verified for the green paints of *Martyrology* (Lv. 16, f. 59 v), *Sermones de Tempore*, *Setentiae* by São Bernardo (Alc. 358, f. 1) and *Homiliae in* Leviticum, *Numerum*, *Josue et Judices* by Orígines (Alc. 360, f. 2). The green paint of *Lectionary* (Lv. 13, f. 44 v) presents a case where this collapse and possible complexation did not occur, so the historical sample maintains the amide I and II bands at 1653 cm^{-1} and 1541 cm^{-1}, respectively, as well as defined bands corresponding to the CH stretching at 2963 cm^{-1} and 2933 cm^{-1} [33]. For the other three historical greens, the CH bands are less prominent or non-existent in the case of the *Sermones* (Alc. 358), which corroborates the possible collapse of the protein.

Alongside the protein bands, two other broad bands appear that seem to be linearly related to the protein–copper complex but were not assigned; the bands are signalled in orange between 1409 and 1412 cm^{-1} and between 781 and 793 cm^{-1}. In the paints, the complexation and possible degradation of the protein are verified, and calcium oxalate is present, characterised by its C–O stretching band at 1322 cm^{-1} and by its band at 784 cm^{-1}. Of the four bottle green paints in Figure 10, only the ones that present the bands corresponding to the copper proteinate complex have calcium oxalate, and this is verified for all the Portuguese bottle green paints studied. This compound results from the degradation of the protein in the presence of a source of calcium. In these paints, the calcium derives from calcium carbonate, identified by the distinctive bands at 876–877 cm^{-1} (δ_{as} CO_3^{2-}) and at 713 cm^{-1} (δ_s CO_3^{2-}). In some examples, as in the green of the *Homiliae* (Alc. 360), the amount of calcium carbonate is higher, and it is possible to identify the stretching of the CO_3^{2-} at 1426 cm^{-1}.

An interesting case was identified in *Martyrology* (Lv. 16), where a similar fingerprint to that of a polysaccharide was observed between 1200 and 1000 cm^{-1}, the region linked to the skeletal C–O and C–C vibrations of glycosidic bonds in polysaccharides [38]. The nature of this signal remains to be clarified; nonetheless, it is helpful to demonstrate that the broad band in the other spectra, at approximately 1079–1080 cm^{-1}, does not originate from a polysaccharide binder, as the structure is entirely different.

In ms24 of the *Books of Hours*, we observe a reflectance maximum at 539 nm, which aligns well with our reproductions of malachite in Figure 9, top (p50 in [47]).

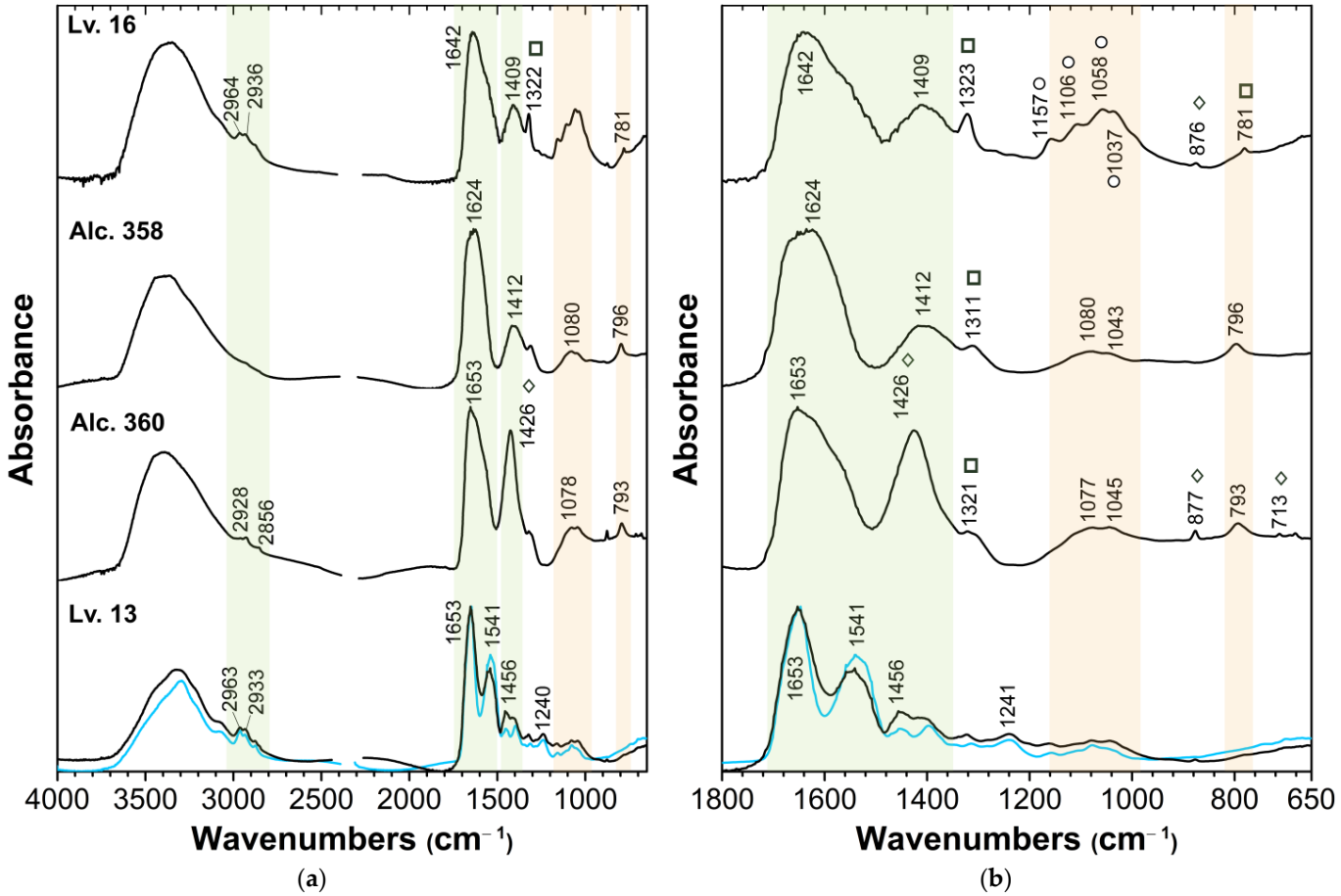

Figure 10. Infrared spectra of bottle green paints (**a**) and the close-up of the fingerprint region (**b**): *Martyrology* (Lv.16), f. 59 v; *Sermones de Tempore*, *Setentiae* by São Bernardo (Alc 358), fol.1; *Homiliae in Leviticum*, *Numerum*, *Josue et Judices* by Orígines (Alc. 360), f. 2; and *Temporal Lectionary* (Lv13), f. 44 v, compared to a protein reference (blue). The characteristic bands of the complex are in green, while the unidentified complex-related bands are shown in orange. Calcium carbonate (◊) and calcium oxalate (□) are also detected, along with a possible polysaccharide (○).

3.4. New Challenges for Bottle Green at Soleil

Through analysis using Synchrotron deep UV luminescence, it was possible to determine the extent of oxalates in a historic micro-sample from Alc. 421, f. 181; see Figures 11 and 12. The areas marked in red represent the oxalates, which cover most of the paint, indicating that binder degradation affects the entire surface. This may be at the core of the characteristic loss of cohesion observed. Due to fluorescence quenching caused by copper ions, the binder's fluorescence could not be detected; however, a particle corresponding to tryptophan was observed. This particle might be related to egg white or egg yolk that could have been used in the mixture with the binder or as a varnish. In Figure 12, a calcium oxalate sample is compared with the bottle green from Alc 421, f. 181, showing that it is possible to match.

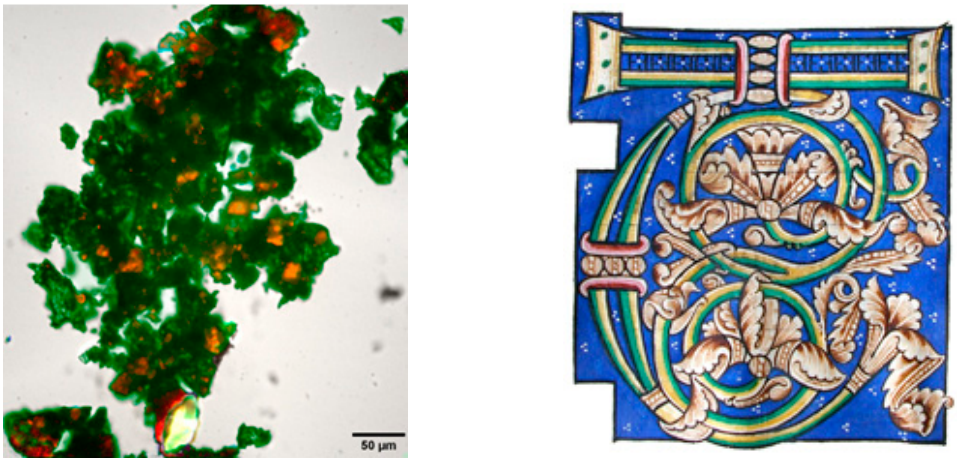

(**a**) micro-sample (**b**) MS Alc. 421, f. 181

Figure 11. Synchrotron deep UV luminescence image from microsamples of bottle green (**a**) taken from (**b**) an initial of MS Alc. 421, f. 181 (scale in 50 micrometres). In this initial, the blue colour is from lapis lazuli paint, with lac dye paints also used, and a tempera made from glair emphasises the parchment's colour.

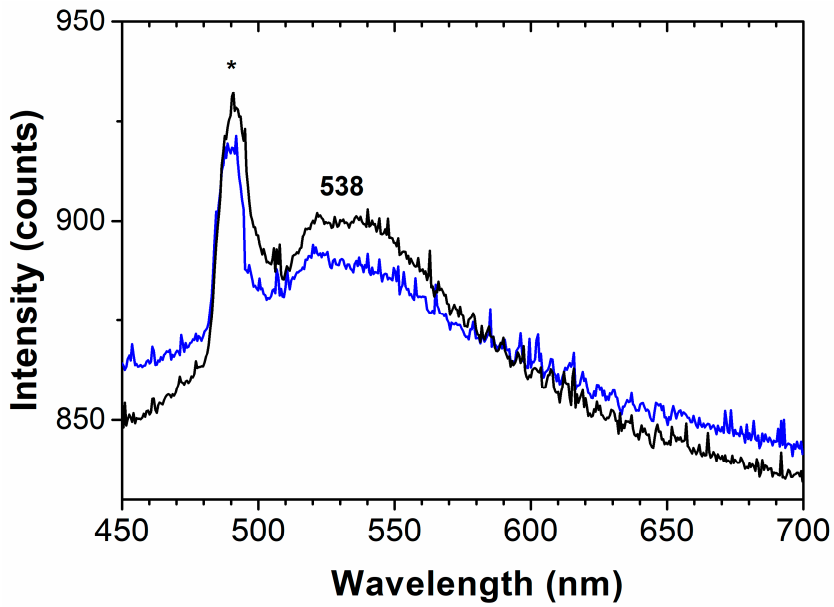

Figure 12. Emission spectrum of calcium oxalate reference is shown in blue, compared with bottle green from Alc 421 f. 181, black line. The star is an artefact. Acquired at Soleil Synchrotron; for more details, please see Synchrotron deep UV photoluminescence.

4. Discussion

The historical importance of three key pigments in medieval times—namely, bottle green, verdigris, and malachite—cannot be overstated. Bottle green, a synthetic copper proteinate, is a pigment about which we are continually discovering new information. Its presence has been positively identified in an 11th–12th century codex from Fécamp Abbey [14], in Portuguese monastic production (12th–13th c) [35] and in the scriptorium of Alfonso X, king of the Crown of Castile (r. 1252–1284) [37]. Malachite, another important pigment, was commonly used in Books of Hours and has been accurately identified. MicroFTIR, an essential tool for pigment identification, plays a vital role in accurately recognising all these pigments. Reflectance spectroscopy in the mid-infrared also significantly aids their identification, offering a comprehensive understanding of structure, composition and degradation patterns. Similarly, FORS in the NIR and visible range provides valuable

insights, further enhancing our knowledge. These spectroscopy techniques are crucial in our research and significantly contribute to our understanding of the historical pigments. In medieval manuscript illuminations, verdigris has been harder to detect, possibly because it tends to degrade over time.

5. Conclusions

The spectroscopic techniques employed in this study enable pigment identification and chemical analysis [34,35,50]. They align with the "do no harm" conservation principle by protecting fragile manuscripts and artefacts from damage. Moreover, spectroscopy can detect early signs of deterioration, like verdigris browning or malachite darkening, before visible problems appear.

Early problem detection enables preventive conservation, which is more sustainable than frequent restorations or replacements. Understanding the exact chemical composition of pigments helps choose compatible restoration materials and reduce reactions that could accelerate decay. This approach decreases waste and the necessity for repeated interventions, ultimately extending the lifespan of artworks.

Furthermore, protecting these pigments involves raising public awareness. Educating conservators, curators, and museum directors about their importance promotes their preservation. Such collective efforts are essential to safeguarding our cultural heritage.

Author Contributions: Investigation, M.S., M.P., G.B., M.V., F.J., P.N. and M.J.M.; writing—original draft preparation, M.S., M.P., G.B., M.V. and M.J.M.; writing—review and editing, M.S., M.P., G.B., M.V., P.N. and M.J.M.; supervision, F.J.; funding acquisition. All authors have read and agreed to the published version of the manuscript.

Funding: This work was funded by national funds from FCT—Fundação para a Ciência e a Tecnologia, I.P., under the scope of the projects UID/50006/2025, UID/PRR/50006/2025 and LA/P/0008/2020 of the Associated Laboratory for Green Chemistry—LAQV REQUIMTE (https://doi.org/10.54499/UID/50006/2025, https://doi.org/10.54499/UID/PRR/50006/2025; Paula Nabais trough 2021.01344.CEECIND/CP1657/CT0028.

Data Availability Statement: Further research data may be provided by the authors Maria J. Melo and Marcello Picollo.

Acknowledgments: The authors wish to thank the staff and directory board of the Biblioteca Nacional de Portugal (BNP), Biblioteca Pública Municipal do Porto (BPMP), Biblioteca do Palácio Nacional da Ajuda, Palácio Nacional de Mafra (PNM), and National Institute Archives/Torre do Tombo (IAN-TT) for their generous support and collaboration.

Conflicts of Interest: The authors declare no conflicts of interest.

References

1. Prati, S.; Bonacini, I.; Sciutto, G.; Genty-Vincent, A.; Cotte, M.; Eveno, M.; Menu, M.; Mazzeo, R. ATR-FTIR microscopy in mapping mode for the study of and its secondary products. *Appl. Phys. A* **2016**, *122*, 10. [CrossRef]
2. Špec, T.; Retko, K.; Ropret, P.; Meden, A.; Bernard, J. The influence of UV–Vis radiation, and oscillations of temperature and relative humidity, on malachite alteration in the presence of different organic binders and varnishes. *J. Raman Spectrosc.* **2014**, *45*, 1068–1075. [CrossRef]
3. Švarcová, S.; Hradil, D.; Hradilová, J.; Čermáková, Z. Pigments—Copper-based greens and blues. *Archaeol. Anthropol. Sci.* **2021**, *13*, 190. [CrossRef]
4. de la Roja, J.M.; Baonza, V.G.; San Andrés, M. Application of Raman microscopy to the characterization of different verdigris variants obtained using recipes from old treatises. *Spectrochim. Acta Part A Mol. Biomol. Spectrosc.* **2007**, *68*, 1120–1125. [CrossRef]
5. Punis, R.; Veronese, M.; Meneghetti, M.; Zoleo, A. Copper Soaps Formation in Verdigris−Linseed Oil Painting Mixtures: A Multispectroscopic Characterization. *Inorg. Chem.* **2024**, *63*, 4108−4119. [CrossRef]
6. Ricciardi, P.; Pallipurath, A.; Rose, K. 'It's not easy being green': A spectroscopic study of green pigments used in illuminated manuscripts. *Anal. Methods* **2013**, *5*, 3819–3824. [CrossRef]

7. Gilbert, B.; Denoël, S.; Weber, G.; Allart, D. Analysis of green copper pigments in illuminated manuscripts by micro-Raman spectroscopy. *Analyst* **2003**, *10*, 1213–1217. [CrossRef] [PubMed]
8. Salvadó, N.; Pradell, T.; Pantos, E.; Papiz, M.Z.; Molera, J.; Seco, M.; Vendrell-Saz, M.J. Identification of copper-based green pigments in Jaume Huguet's Gothic altarpieces by Fourier transform infrared microspectroscopy and synchrotron radiation X-ray diffraction. *J. Synchrotron Radiat.* **2002**, *9*, 215–222. [CrossRef] [PubMed]
9. Salvadó, N.; Butí, S.; Cotte, M.; Cinque, G.; Pradell, T. Shades of green in 15th century paintings: Combined microanalysis of the materials using synchrotron radiation XRD, FTIR and XRF. *Appl. Phys. A* **2013**, *111*, 47–57. [CrossRef]
10. Knipe, P.; Eremin, K.; Walton, M.; Babini, A.; Rayner, G. Materials and techniques of Islamic manuscripts. *Herit. Sci.* **2018**, *6*, 55. [CrossRef]
11. Naumova, M.M.; Pisareva, S.A.; Nechiporenko, G.O. Green copper pigments of old Russian frescoes. *Stud. Conserv.* **1990**, *35*, 81–88. [CrossRef]
12. Leygraf, C.; Wallinder, I.O.; Tidblad, J.; Graedel, T. *Atmospheric Corrosion*, 2nd ed.; John Wiley & Sons: Hoboken, NJ, USA, 2016; pp. 154–196.
13. Doherty, B.; Daveri, A.; Clementi, C.; Romani, A.; Bioletti, S.; Brunetti, B.; Sgamellotti, A.; Miliani, C. The Book of Kells: A Non-Invasive MOLAB Investigation by Complementary Spectroscopic Techniques. *Spectrochim. Acta Part A Mol. Biomol. Spectrosc.* **2013**, *115*, 330–336. [CrossRef]
14. Coupry, C. Les Pigments Utilisés Por l'enluminure à Fécamp Aus XIe et XIIe Siècles. In *Manuscrits et Enluminures Dans le Monde Normand (Xe–XVe Siècles)*, 1st ed.; Bouet, P., Dosdat, M., Eds.; Presses Universitaires de Caen: Caen, France, 1999; Volume 1, pp. 69–79.
15. Coupry, C. À la recherche des pigments. In *Revista de História da Arte Série w, 1*, 1st ed.; Miranda, A., Melo, M.J., Eds.; Revista de História da Arte: Lisbon, Portugal, 2011; Volume 1, pp. 127–136. Available online: https://revistadehistoriadaarte.wordpress.com/wp-content/uploads/2011/09/art09.pdf (accessed on 24 March 2026).
16. Chang, T.; Wallinder, I.O.; De la Fuente, D.; Chico, B.; Morcillo, M.; Welter, J.-M.; Leygraf, C. Analysis of Historic Copper Patinas. Influence of Inclusions on Patina Uniformity. *Materials* **2017**, *10*, 298. [CrossRef]
17. Frost, R.L.; Martens, W.N.; Kloprogge, J.T.; Williams, P.A. Raman spectroscopy of the basic copper chloride minerals atacamite and paratacamite: Implications for the study of copper, brass and bronze objects of archaeological significance. *J. Raman Spectrosc.* **2002**, *33*, 801–806. [CrossRef]
18. Buse, J.; Otero, V.; Melo, M.J. New Insights into Synthetic Copper Greens: The Search for Specific Signatures by Raman and Infrared Spectroscopy for Their Characterization in Medieval Artworks. *Heritage* **2019**, *2*, 1614–1629. [CrossRef]
19. Frost, R.L.; Williams, P.A.; Martens, W.; Leverett, P.; Kloprogge, J.T. Raman spectroscopy of basic copper (II) and some complex copper (II) sulfate minerals: Implications for hydrogen bonding. *Am. Miner.* **2004**, *89*, 1130–1137. [CrossRef]
20. Nevin, A.; Melia, J.L.; Osticioli, I.; Gautier, G.; Colombini, M.P. The identification of copper oxalates in a 16th century Cypriot exterior wall painting using micro FTIR, micro Raman spectroscopy and Gas Chromatography-Mass Spectrometry. *J. Cult. Herit.* **2008**, *9*, 154–161. [CrossRef]
21. Nakamoto, K. *Infrared and Raman Spectra of Inorganic and Coordination Compounds, Theory and Applications in Inorganic Chemistry*, 6th ed.; Wiley-Interscience: Hoboken, NJ, USA, 2009.
22. Buti, D.; Rosi, F.; Brunetti, B.G.; Miliani, C. In-situ identification of copper-based green pigments on paintings and manuscripts by reflection FTIR. *Anal. Bioanal. Chem.* **2013**, *405*, 2699–2711. [CrossRef] [PubMed]
23. Monico, L.; Rosi, F.; Miliani, C.; Daveri, A.; Brunetti, B.G. Non-invasive identification of metal-oxalate complexes on polychrome artwork surfaces by reflection mid-infrared spectroscopy. *Spectrochim. Acta Part A Mol. Biomol. Spectrosc.* **2013**, *116*, 270–280. [CrossRef]
24. Hawthorne, J.G.; Smith, C.S. *Theophilus on Divers Arts: The Foremost Medieval Treatise on Painting, Glassmaking, and Metalwork*, 3rd ed.; Dover Publications: New York, NY, USA, 1979; pp. 35–41.
25. Strolovitch, D.L. Old Portuguese in Hebrew Script: Convention, Contact, and Convivência. Ph.D. Thesis, Cornell University, Cornell, WI, USA, 2005.
26. Clarke, M. *Mediaeval Painters' Materials and Techniques: The Montpellier Liber Diversarum Arcium*, 1st ed.; Archetype: London, UK, 2011; p. 112.
27. Merrifield, M.P. *Medieval and Renaissance Treatises on the Arts of Painting: Original Texts with English Translations*, 1st ed.; Dover: Mineola, NY, USA, 2013; pp. 273, 706.
28. Frost, R.L.; Yang, J.; Ding, Z. Raman and FTIR spectroscopy of natural oxalates: Implications for the evidence of life on Mars. *Chin. Sci. Bull.* **2003**, *48*, 1844–1852. [CrossRef]
29. Martens, W.N.; Frost, R.L.; Williams, P.A. Raman and infrared spectroscopic study of the basic copper chloride minerals—Implications for the study of the copper and brass corrosion and "bronze disease". *Neues Jahrb. Für Mineral.-Abh.* **2003**, *178*, 197–215. [CrossRef]

30. Scott, D.A.; Taniguchi, Y.; Koseto, E. The verisimilitude of verdigris: A review of the copper carboxylates. *Rev. Conserv.* **2001**, *2*, 73–91. [CrossRef]
31. Salvadó, N.; Butí, S.; Nicholson, J.; Emerich, H.; Labrador, A.; Pradell, T. Identification of reaction compounds in micrometric layers from gothic paintings using combined SR-XRD and SR-FTIR. *Talanta* **2009**, *79*, 419–428. [CrossRef]
32. Otero, V.; Vilarigues, M.; Carlyle, L.; Cotte, M.; De Nolf, W.; Melo, M.J. A little key to oxalate formation in oil paints: Protective patina or chemical reactor? *Photochem. Photobiol. Sci.* **2018**, *17*, 266–270. [CrossRef]
33. Miguel, C. Le vert et le Rouge: A Study on the Materials, Techniques and Meaning of the Green and Red Colours in Medieval Portuguese Illuminations. Ph.D. Thesis, NOVA University Lisbon, Lisbon, Portugal, 2012. Available online: http://run.unl.pt/handle/10362/9304 (accessed on 24 March 2026).
34. Melo, M.J.; Castro, R.; Miranda, A. Colour in Medieval Portuguese Manuscripts: Between Beauty and Meaning. In *Science and Art: The Painted Surface*, 1st ed.; Sgamellotti, A., Brunetti, B.G., Miliani, C., Eds.; Royal Society of Chemistry: Cambridge, UK, 2014; Volume 1, pp. 170–192.
35. Melo, M.J.; Araújo, R.; Castro, R.; Casanova, C. Colour degradation in medieval manuscripts. *Microchem. J.* **2016**, *124*, 837–844. [CrossRef]
36. Clarke, M. *Middle English Recipes for Painters, Stainers, Scribes and Illuminators*, 1st ed.; Oxford University Press: Oxford, UK, 2016.
37. Vieira, M.; Melo, M.J.; Nabais, P.; Lopes, J.A.; Lopes, G.V.; Fernández Fernández, L. The Colors in Medieval Illuminations through the Magnificent Scriptorium of Alfonso X, the Learned. *Heritage* **2024**, *7*, 272–300. [CrossRef]
38. Vieira, M.; Melo, M.J.; de Carvalho, L.M. Towards a sustainable preservation of medieval colors through the identification of the binding media, the medieval tempera. *Sustainability* **2024**, *16*, 5027. [CrossRef]
39. Picollo, M.; Bartolozzi, G.; Cucci, C.; Galeotti, M.; Marchiafava, V.; Pizzo, B. Comparative study of Fourier transform infrared spectroscopy in transmission, attenuated total reflection, and total reflection modes for the analysis of plastics in the cultural heritage field. *Appl. Spectrosc.* **2014**, *4*, 389–397. [CrossRef]
40. Picollo, M.; Aceto, M.; Vitorino, T. UV-Vis spectroscopy. *Phys. Sci. Rev.* **2019**, *4*, 20180008. [CrossRef]
41. Miliani, C.; Monico, L.; Fantacci, S.; Romani, A.; Melo, M.J.; Angelin, E.M.; Janssens, K. Recent insights into the photochemistry of artists' pigments and dyes: Towards better understanding and prevention of colour change in works of art. *Angew. Chem. Int. Ed.* **2018**, *57*, 7324–7334. [CrossRef] [PubMed]
42. Melo, M.J.; Otero, V.; Vitorino, T.; Araújo, R.; Muralha, V.S.F.; Lemos, A.; Picollo, M. A Spectroscopic Study of Brazilwood Paints in Medieval Books of Hours. *Appl. Spectrosc.* **2014**, *68*, 434–444. [CrossRef]
43. Bacci, M.; Baldini, F.; Carlà, R.; Linari, R. A color analysis of the Brancacci Chapel frescoes. *Appl. Spectrosc.* **1991**, *1*, 26–31. [CrossRef]
44. Lever, A.B.P. *Inorganic Electronic Spectroscopy*; Elsevier: Tokyo, Japan; Amsterdam, The Netherlands; Oxford, UK; New York, NY, USA, 1987.
45. Robinet, L.; Heu-Thao, S.; Galante, G.; Latour, G.; Tournié, A.; Daher, C.; Dan, A.; Schanne-Klein, M.C.; Michelin, A.; Deschaux, J. The *Mappa mundi* of Albi: Insight into the manufacturing, life and conservation state of an 8th century world map. *J. Cult. Herit.* **2025**, *74*, 341–352. [CrossRef]
46. Melo, M.J.; Vieira, M.; Nabais, P.; Neves, A.; Pamplona, M.; Angelin, E.M. A Closer Look at Heritage Systems from Medieval Colors to Modern and Contemporary Artworks. *Heritage* **2024**, *7*, 5476–5494. [CrossRef]
47. Araújo, R. Os Livros de Horas (séc. XV) na Colecção do Palácio Nacional de Mafra: Estudo e Conservação. Master's Thesis, NOVA School of Science and Technology (FCT NOVA), Caparica, Portugal, 5 December 2012.
48. Gražėnaitė, E.; Kiuberis, J.; Beganskienė, A.; Senvaitienė, J.; Kareiva, A. XRD and FTIR characterisation of historical green pigments and their lead-based glazes. *Chemija* **2014**, *25*, 199–205. [CrossRef]
49. Jamme, F.; Villette, S.; Giuliani, A.; Rouam, V.; Wien, F.; Lagarde, B.; Réfrégiers, M. Synchrotron UV fluorescence microscopy uncovers new probes in cells and tissues. *Microsc. Microanal.* **2010**, *16*, 507–514. [CrossRef]
50. Bertrand, L.; Gervais, C.; Masic, A.; Robbiola, L. Paleo-inspired systems: Durability, sustainability, and remarkable properties. *Angew. Chem. Int. Ed.* **2018**, *57*, 7288–7295. [CrossRef]